

# Particle Identification with the ATLAS Transition Radiation Tracker

Elizabeth Hines on behalf of the ATLAS collaboration

Department of Physics and Astronomy, University of Pennsylvania, Philadelphia, PA, USA

The ATLAS Transition Radiation Tracker (TRT) is the outermost of the three sub-systems of the ATLAS Inner Detector at the Large Hadron Collider at CERN. In addition to its tracking capabilities, the TRT provides particle identification (PID) ability through the detection of transition radiation X-ray photons. The latter functionality provides substantial discriminating power between electrons and hadrons in the momentum range from 1 to 200 GeV. These proceedings present the commissioning of TRT PID during early 2010 7 TeV data taking. Performance in 2010 and 2011 demonstrating the TRT's ability to identify electrons, complementary to calorimeter based identification methods, will also be shown.

## 1. Introduction and the Transition Radiation Tracker

The ATLAS Inner Detector (ID) is composed of three detector sub-systems: the silicon-based Pixel and SemiConductor Tracker (SCT) detectors, and the gaseous drift tube Transition Radiation Tracker (TRT) [1]. The TRT is the outermost of the three sub-systems. It employs a unique design which combines tracking measurements with particle identification based on detection of transition radiation (TR). The detection of TR allows for discrimination between electrons and pions over the energy range 1-200 GeV and is a crucial component of the electron selection criteria in ATLAS [2][3]. These proceedings present the particle identification (PID) performance of the TRT observed in  $\sqrt{s} = 7$  TeV proton-proton collision data collected with the ATLAS detector at the Large Hadron Collider (LHC) in 2010.

The TRT is a straw tracker composed of 298,304 carbon-fiber reinforced Kapton straws, arranged in a barrel and two symmetrical end-cap configurations [4]. The barrel section covers  $560 < R < 1080$  mm and  $|z| < 720$  mm and has the straws aligned with the direction of the beam axis [5].<sup>1</sup> The two end-cap sections cover  $827 < |z| < 2744$  mm and  $617 < R < 1106$  mm and have the straws arranged in planes composing wheels, aligned perpendicular to the beam axis, pointing outwards in the radial direction [6]. The TRT extends to pseudo-rapidity  $|\eta| = 2$ . The average number of TRT hits per track is around 34, except in the transition region between barrel and end-caps and at the edge of the acceptance ( $|\eta| \lesssim 1.7$ ) Polypropylene fibers interwoven between straw layers are used in the barrel for radiator material and regular polypropylene foils in the end-caps. The straws are filled with a gas mixture of 70% Xe, 27% CO<sub>2</sub> and 3% O<sub>2</sub>. Xenon was chosen for its high efficiency to absorb TR photons of typical energy 6–15 keV.

The TRT operates as a combination drift chamber and TRD, employing two adjustable thresholds, a low-threshold (LT) of about 300 eV and a high-threshold (HT) of about 6-7 keV [7] in its front-end electronics. The two thresholds allow for simultaneous measurement of tracking information and identification of characteristic large energy deposits due to the absorption of TR photons.

## 2. Data samples

Data from proton-proton collisions at the LHC at  $\sqrt{s} = 7$  TeV recorded by the ATLAS detector in 2010 were used for the studies reported in these proceedings. The detector response for electrons was studied with samples of reconstructed photon conversions and Z boson decays. The detector response to pions was studied using the same minimum-bias data set as for photon conversions.

A minimum bias trigger was used to record the data set used for the reconstruction of photon conversions and pion candidates. During the initial low-luminosity running period from April 15 to June 5, 2010, the events were collected at a rate that was typically between 40Hz and 200Hz, providing a high statistics sample of electrons from photon conversions. This data set corresponds to an integrated luminosity of approximately  $\mathcal{L}$

<sup>1</sup>ATLAS uses a right-handed coordinate system with its origin at the nominal interaction point (IP) in the center of the detector and the z-axis coinciding with the axis of the beam pipe. The x-axis points from the IP to the center of the LHC ring, and the y-axis points upward. Cylindrical coordinates (R,  $\phi$ ) are used in the transverse plane,  $\phi$  being the azimuthal angle around the beam pipe and R, the distance from the IP in the radial direction. The track pseudo-rapidity is defined as  $\eta = -\ln(\theta/2)$ , where the polar angle  $\theta$  is the angle between the track direction and the z axis

$= 9 \text{ nb}^{-1}$ . Data recorded by an efficient electron trigger from June 24, 2010 - October 29, 2010, corresponding to an integrated luminosity of  $\mathcal{L} = 35 \text{ pb}^{-1}$ , was used to reconstruct electron candidates from Z boson decays.

The LHC bunch spacing during both running periods was 150 ns or greater. Pile-up from multiple interactions per bunch crossing was small. The average number of minimum bias interactions per beam crossing was less than 0.2 in the data set used for photon conversions, and about three in the data set used to reconstruct the sample of Z bosons.

The results observed in data were compared to Monte Carlo (MC) simulations [8]. The detector response to electrons from photon conversions and pions in data were compared to *Pythia* non-diffractive minimum bias MC simulation. The electrons from Z boson decays were compared to *Pythia*  $Z \rightarrow e^+e^-$  MC simulation.

## 2.1. Electron and pion candidates

Photon conversions to electron-positron pairs were used to reconstruct a pure sample of electrons in early data. The photon conversion candidates [9] are required to have two tracks, each with a minimum of 20 TRT hits and four silicon (SCT and Pixel) hits. The conversion vertex is required to be well reconstructed and to be at least 60 mm away from the primary vertex in the radial direction. To improve the sample purity, a tag and probe method is applied; the tag leg is required to have a ratio of the number of TRT high-threshold hits to total TRT hits of at least 0.12. Over 500,000 electron candidates satisfy these selection criteria, providing a high statistics sample of electron candidates.

A second sample of electron candidates is obtained from the reconstruction of  $Z \rightarrow e^+e^-$  decays. Electrons from this sample have higher momenta, and can thus be used to probe the TR performance at higher values of  $\gamma$ . Electron candidates are required to pass the calorimeter based “medium” electron selection criteria [2], and to have an innermost Pixel layer (b-layer) hit. Candidate events are required to have two such electrons, with a reconstructed di-lepton invariant mass in the range 75 – 105 GeV, based on measurements from their calorimeter clusters. Again, one tag leg is required to have a TRT high-threshold ratio greater than 0.12, and both legs are required to have at least 20 TRT hits.

Pion candidates are selected from reconstructed particle tracks that have a minimum of 20 TRT and four silicon hits. Further selection criteria are applied to reject electrons, protons and kaons. Any track that does not have a hit in the innermost Pixel layer or that is reconstructed as a part of a photon conversion candidate is excluded. In addition, any track with a measured  $dE/dx$  above  $1.6 \text{ MeVg}^{-1}\text{cm}^2$  in the Pixel detector is excluded in order to reduce the contamination from protons (and to a lesser extent kaons) at low momentum.

## 3. Transition radiation and high-threshold hits

Figure 1 shows the HT fraction distributions for electron and pion candidates. The HT fraction is defined as the ratio hits on track that exceed the high threshold to the total number of hits on track. The distribution for electrons is clearly shifted to higher values. This value is defined on a per track basis, whereas the high-threshold probability is defined as the total number of high-threshold hits summed over all candidates divided by the total number of hits summed over all candidates. The following sections show the HT dependence on the  $\gamma$  factor, and performance of a requirement on the HT fraction, in terms of the electron efficiency and pion misidentification probability. Finally, validation of hardware settings with 7 TeV collision data are presented.

### 3.1. Transition radiation onset

The first step towards establishing electron identification with the TRT is to observe the expected increase in the average number of HT hits with  $\gamma$ . The increase has been observed in 2004 test-beam data [13], cosmic-ray data [14] and for collision data at  $\sqrt{s} = 900 \text{ GeV}$  [15]. The HT probability observed in 7 TeV collision data is shown in Fig. 2 and is consistent with earlier measurements. The results are shown separately for several intervals in pseudo-rapidity  $\eta$  reflecting different detector regions. The errors shown are statistical only. For the electron candidates, the sharp turn-on of the transition radiation can be seen, with the HT probability increasing rapidly from 0.05 to a plateau of 0.2–0.3 depending on  $\eta$  region. The HT plateau level in the end-cap region is higher than in the barrel. Electrons from the reconstructed Z decays allow studies of HT probability at  $\gamma \sim 10^5$ , which can not be accessed with electrons from photon conversions.

The pion candidates shown in Fig. 2 populate the region  $\gamma < 10^3$ . In this  $\gamma$  range, HT hits are caused by large ionization energy deposits due to Landau  $dE/dx$  fluctuations. The HT probability for pion candidates increases gradually from about 0.04 at  $\gamma \sim 1$  to about 0.07 at  $\gamma \sim 700$  ( $p \sim 100 \text{ GeV}$ ) due to the rise of  $\langle dE/dx \rangle$

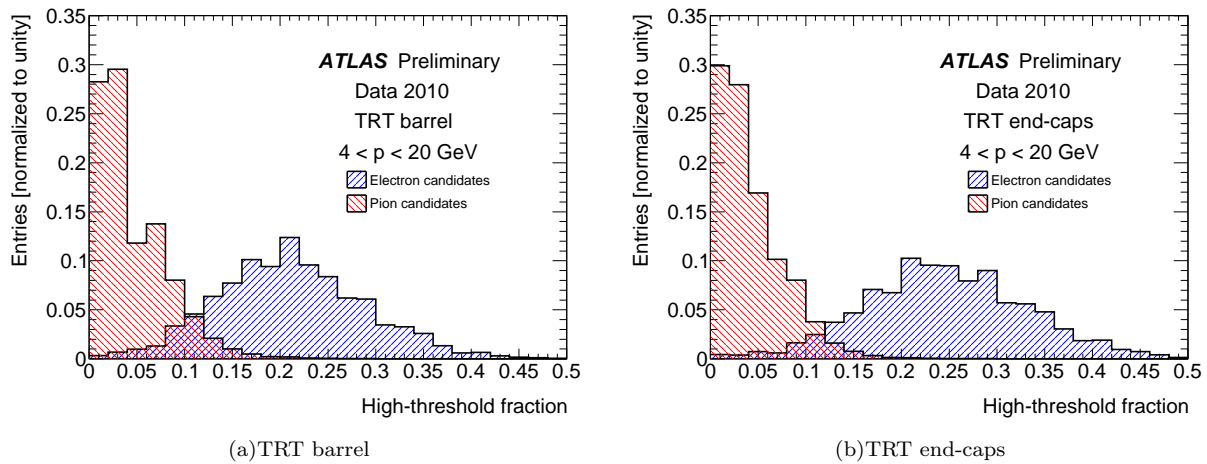
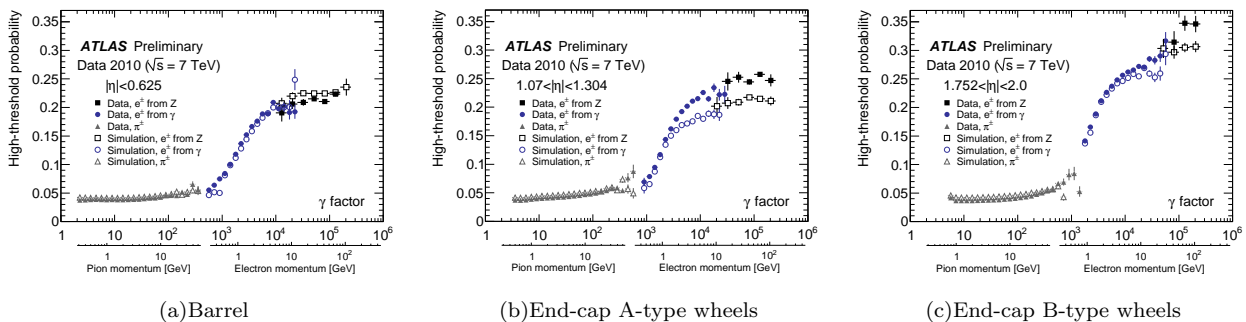


Figure 1: The HT fraction for electron and pion candidates[3]

with increasing track momentum. This behavior was cross-checked with a sample of pion candidates from  $K_s^0$  decays that has higher pion purity, and the results were in good agreement.


 Figure 2: The high-threshold turn on curve, separated into detector regions by track  $\eta$ [3]

### 3.2. Electron efficiency and pion misidentification probability

The HT-based electron-pion separation demonstrated in Fig. 1 is utilized by a requirement of a minimum HT fraction for electron identification. Figure 3(a) shows the fraction of electron candidates that pass a HT fraction selection requirement, for different  $|\eta|$  regions. The pion misidentification probability  $p_{\pi \rightarrow e}$  is the probability for a pion to pass an electron HT fraction selection criteria and is shown in Fig. 3(b). The pion rejection power is  $1/p_{\pi \rightarrow e}$ . A direct comparison of the electron efficiency and pion misidentification probability is shown in Fig. 4. A benchmark point of a cut on high-threshold fraction that has a 90% electron efficiency is used. The uncertainty on the pion misidentification probability shown in Fig. 4 was estimated by varying the selection criteria such that the electron efficiency changed by  $\pm 2\%$ . The range of  $\pm 2\%$  is sufficiently big to include the uncertainties due to hadron contamination in the electron sample of about 1%.

### 3.3. Validation of hardware settings

In order to determine the optimal average high threshold setting, data corresponding to an integrated luminosity of  $20 \text{ nb}^{-1}$  was taken with different HT settings in July 2010. An electron trigger that maximized the number of reconstructed photon conversion candidates was used to record these data.

The value of the high threshold can be varied by changing the Digital to Analogue Converter setting (DAC counts) on the Amplification, Shaping, Discrimination, and Base-Line Restoration (ASDBLR) chip [7], in steps of about 60 eV. Prior to the start of collision data-taking, the average HT was adjusted to the setting that gave

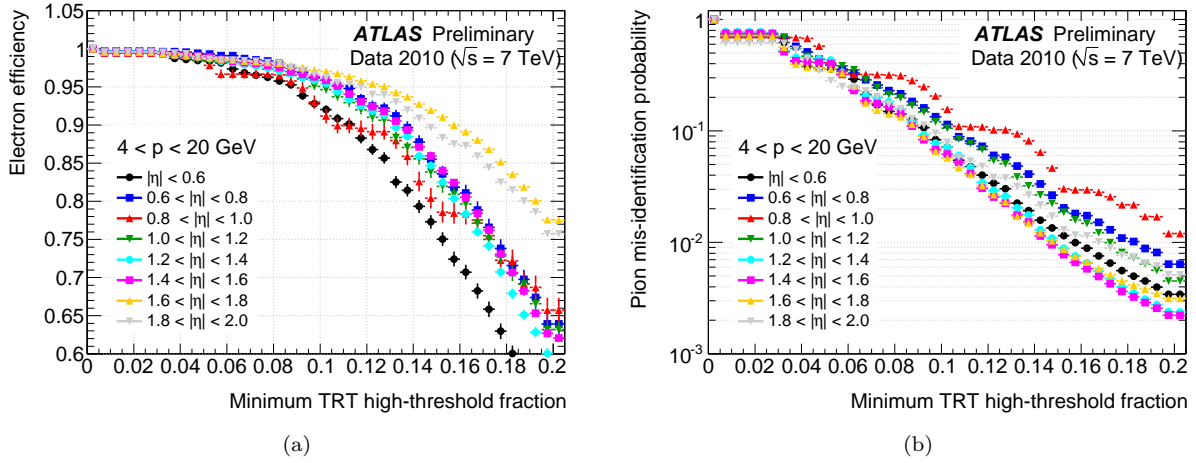


Figure 3: The fraction of electron (a) and pion (b) candidates that pass a cut on high-threshold fraction.[3]

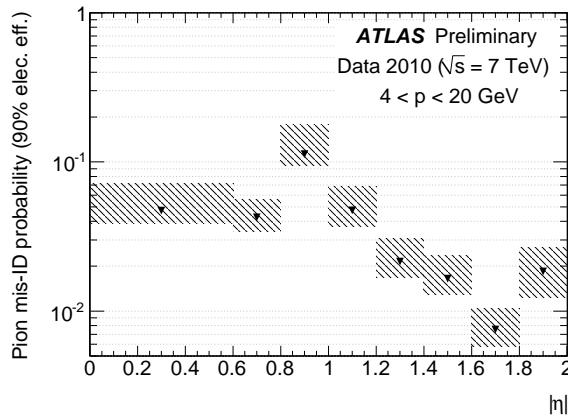


Figure 4: Pion mis-ID probability for the HT fraction criteria that gives 90% electron efficiency.[3]

the best performance at the test beam. Results from electronics noise scans were used to correct for the large variations in response due to variations in ground offsets.

To validate the average HT setting, data were recorded with six different HT settings: nominal settings,  $\pm 15$  DAC counts from nominal,  $\pm 25$  DAC counts from nominal, and  $+8$  DAC counts from nominal. The high-threshold settings were varied uniformly across the entire detector.

As the threshold is decreased, the HT probability increases for both electron and pion candidates. The optimal average HT setting is determined based on the pion rejection power. The HT fraction selection criteria that gives 90% electron efficiency was determined for different values of high threshold settings and for different  $\eta$  bins. Figure 5 shows the efficiency for a pion candidate to pass the selection criteria as a function of the high threshold setting difference. For all regions, the pion misidentification probability  $p_{\pi \rightarrow e}$  is independent of the HT setting in the range of  $-25$  to nominal DAC count. For settings higher than nominal,  $p_{\pi \rightarrow e}$  increases. Based on these results, the high-threshold was lowered by eight DAC counts across the detector for 2011 data-taking. The primary reason for lowering the thresholds was to operate at stable settings, where the performance does not vary much if the HT is slightly above or below the nominal.

## 4. Summary

Studies in the early collision data collected with the ATLAS detector have confirmed that electron identification based on transition radiation measured by the TRT is performing well, and in some detector regions even exceeds the performance obtained from the current detector simulation. The pion misidentification probability

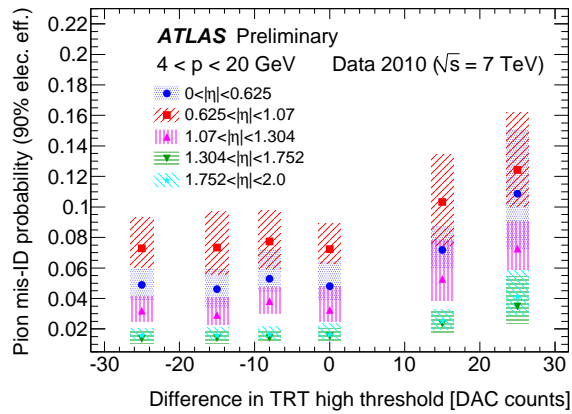


Figure 5: Pion mis-ID probability at 90% electron efficiency as a function of hardware settings for different  $\eta$  ranges.[3]

for selection criteria that give 90% electron efficiency is about 5% (rejection factor 20) for the majority of the detector and as low as 1-2% in the best performing detector regions. Analysis of data from a dedicated run with different hardware settings confirmed that the thresholds were close to their optimal value, and only small adjustments were made in order to ensure stable performance under a wide range of operating conditions. The transition radiation measurement was used to identify electrons for the first W boson production cross section measurement by ATLAS [17], as well as for the  $W^+W^-$  cross section measurement [18] and other analyses such as a search for supersymmetry [19].

## References

- 1 ATLAS Collaboration, *The ATLAS Experiment at the CERN Large Hadron Collider*, JINST **3**, S08003 (2008).
- 2 ATLAS Collaboration, *Electron performance measurements with the ATLAS detector using 2010 LHC proton-proton collision data*, ATLAS note CERN-PH-EP-2011-117
- 3 ATLAS Collaboration, *Particle Identification Performance of the ATLAS Transition Radiation Tracker*, ATLAS note ATLAS-CONF-2011-128 <https://cdsweb.cern.ch/record/1383793>
- 4 E. Abat et al., *The ATLAS Transition Radiation Tracker (TRT) proportional drift tube: design and performance*, JINST **3**, P02013 (2008).
- 5 E. Abat et al., *ATLAS TRT Barrel Detector*, JINST **3**, P02014 (2008).
- 6 E. Abat et al., *The ATLAS TRT end-cap detectors*, JINST **3**, P10003 (2008).
- 7 E. Abat et al., *The ATLAS TRT electronics*, JINST **3**, P06007 (2008).
- 8 ATLAS Collaboration, *The ATLAS Simulation Infrastructure*, Eur. Phys. J. **C70**, 823-874 (2010).
- 9 ATLAS collaboration, *Photon Conversions at  $\sqrt{s} = 900$  GeV measured with the ATLAS Detector*, ATLAS note ATLAS-CONF-2010-007 <http://cdsweb.cern.ch/record/1274001>.